

ADVANCED EVALUATIONS OF DISPLACEMENT AND GAS PRODUCTION CROSS SECTIONS FOR CHROMIUM, IRON, AND NICKEL UP TO 3 GEV INCIDENT PARTICLE ENERGY

A.Yu.Konobeyev, U.Fischer

Karlsruhe Institute of Technology, Institute for Neutron Physics and Reactor Technology, Hermann-von-Helmholtz-Platz 1, Eggenstein-Leopoldshafen, 76344 Germany, alexander.konobeev@kit.edu; ulrich.fischer@kit.edu

L.Zanini

Paul Scherrer Institut, CH-5232 Villigen PSI, Switzerland, luca.zanini@psi.ch

Displacement cross-sections, hydrogen- and helium-isotope production cross-sections were evaluated for chromium, iron, and nickel for incident neutron and proton energies up to 3 GeV. Various models including the nuclear optical model, the pre-compound exciton model, and the intranuclear cascade evaporation model were used for calculations of cross-section and energy particle and recoil distributions. The binary collision approximation model and results of molecular dynamics simulations were applied to get the number of generated defects in materials.

I. INTRODUCTION

The study of the radiation induced damage of stainless steel employed in the design of spallation neutron sources and accelerators requires a detailed knowledge of displacement and gas production cross-section data for a wide energy range of primary nucleons. The use of rough approximations for the calculations of the number of radiation defects based e. g. on the NRT model^{1,2}, and of simplified approaches for the description of the cluster emission in standard nuclear model codes³, in general result in severe disagreement with experimental data.

In the present work neutron and proton induced displacement cross-sections were calculated for the main components of stainless steels using the binary collision approximation model (BCA) and results of molecular dynamics simulations (MD). Energy distributions of recoils were obtained by optical, pre-equilibrium, and intranuclear cascade evaporation model simulations (and using of other approaches). The IOTA code⁴, developed at KIT, Karlsruhe, was applied to obtain the number of defects in irradiated materials.

The evaluation of the gas production cross-sections including separate evaluations of proton-, deuteron-, triton-, ³He-, and ⁴He- production cross-sections was performed on the basis of nuclear model calculations, available experimental data, and systematics predictions.

The contributions of non-equilibrium cluster emission to the gas production cross-sections were calculated using the geometry dependent hybrid model, phenomenological pick-up, coalescence and knock-out models (and other approaches).

II. DISPLACEMENT CROSS-SECTIONS

The general expression for the displacement cross-section can be written as follows

$$\sigma_d(E_n) = \sum_i \int_{E_d}^{T_i^{\max}} \frac{d\sigma(E_n, Z_T, A_T, Z_i, A_i, T_i)}{dT_i} \times \eta(Z_T, A_T, Z_i, A_i, T_i) N_{\text{NRT}}(Z_T, A_T, Z_i, A_i, T_i) dT_i \quad (1)$$

where E_n is the incident particle energy; $d\sigma/dT_i$ is the energy distribution of i -th primary knock-on atom (PKA); Z and A are the atomic and the mass numbers, “ T ” and “ i ” relates to the target and the recoil atom, correspondingly (for the elastic scattering $Z_i = Z_T$, $A_i = A_T$); N_{NRT} is the number of Frenkel pairs predicted by the NRT model^{2,3}: $N_{\text{NRT}} = 0.8 \cdot T_{\text{dam}} / (2E_d)$; T_{dam} is the “damage energy” equal to the energy transferred to lattice atoms reduced by the losses for electronic stopping of atoms in the displacement cascade; η is the defect production efficiency⁵; E_d is the effective threshold displacement energy equal to 40 eV for all materials considered here; T_i^{\max} is the maximal kinetic energy of the PKA produced in i -th reactions; the summation is over all recoil atoms produced in the irradiation.

The method of the calculation of the number of displacements is briefly described below. The details can be found in Refs.6-9. The BCA model is applied for the simulation of atomic collision for an ion moving in the material up to its certain minimal kinetic energy (T_{crit}). Below this energy the BCA simulation is interrupted and the number of defects is estimated using results of MD calculations. In the present work the number of defects produced by ions with the kinetic energy below T_{crit} was

estimated for chromium and iron according to MD simulations of Vörtler et al.¹⁰, and for nickel according to Bacon et al.¹¹. The energy T_{crit} was taken about 61 keV, which corresponds to the “critical” damage energy equal to 40 keV for all considered materials. The last value is considered as the highest energy where the results of MD simulations^{10,11} can be applied. The BCA calculations were performed using the IOTA code⁴.

The efficiency of the defect generation $\eta(T)$ is shown in Fig.1 for the self-ion irradiation of iron depending on the PKA energy. The discussion of the form of the energy dependence of $\eta(T)$ can be found in Ref.8.

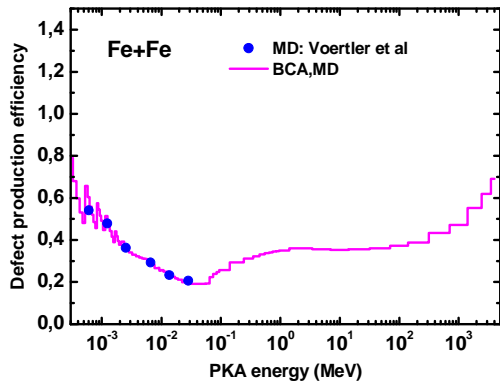


Fig. 1: The efficiency of the defect production for the Fe-Fe irradiation obtained using the combined BCA,MD method and results of the MD simulation¹⁰.

The displacement cross-section is calculated as the sum of displacement cross-sections corresponding to the proton or neutron elastic scattering σ_{del} and the displacement cross-section for nucleon nonelastic interactions with target material σ_{dnon} .

The calculation of σ_{del} for incident protons with energies up to several MeV has been performed using the formula for the recoil energy distribution taking into account screening effects in the ion scattering in materials⁸. At incident proton energies above 4 MeV the displacement cross-section σ_{del} has been calculated using the optical model with Koning, Delaroche¹², and Madland¹³ potentials. Above the highest projectile energy adopted for optical model calculations using the potential from Ref.13 the calculation of σ_{del} has been performed with the help of the relativistic approach (see details in Ref.8). The elastic displacement cross-section for neutrons has been obtained using the optical model with potentials from Refs.12,13. The σ_{del} displacement cross-section calculated using various models and approaches are in a good agreement in ranges of shared applicability^{8,9,14}.

The evaluation of displacement cross-sections for nonelastic interactions includes the simulation of nuclear

reactions resulting to PKAs with various Z,A, and kinetic energies and the modeling of the displacements production initiated by various PKAs using the combined BCA,MD method as described above.

The recoil energy, Z-, and A-distributions of atoms produced in nuclear interactions of target atoms with primary particles were calculated using nuclear models implemented in MCNPX¹⁵, CASCADE¹⁶, and DISCA-C¹⁷ codes, some details are given in Section 3. Atomic collisions were simulated by BCA,MD approach with the help of the IOTA code⁴. The examples of the displacement cross-section calculated for proton nonelastic interactions with natural nickel are shown in Tables 1-4 at various primary energies. The set of nuclear models used at various incident projectile energies is different depending on the applicability of models.

An appropriate way of evaluation of σ_{dnon} would be the averaging of cross-sections obtained by different models with the weights proportional to their predictive abilities⁸. However the question about the predictive power of various models concerning recoil energy distributions is still open, therefore equal weights were adopted for all models in the present work.

The evaluation of displacement cross-sections σ_d was performed for natural mixtures of isotopes for chromium, iron, and nickel at the incident energy up to 3 GeV. At energies below 20 MeV nuclear data used to obtain recoil energy distributions were taken from ENDF/B-VII. Data were processed using the modified version of the NJOY code including the results of defect production efficiency $\eta(T)$ calculations performed with BCA,MD.

Inconsistencies in nonelastic cross-sections observed in MCNPX calculations at several hundred MeV were eliminated in the σ_{dnon} evaluation.

Two data sets of displacement cross-sections were prepared for each target material using BCA,MD simulations and the NRT model. Data were stored in the ENDF-6 format. The MF file number 3 and MT section numbers 900 and 901 were used to record displacement cross-sections obtained using the BCA,MD approach and NRT, correspondingly.

Fig. 2 shows the evaluated displacement cross-sections for proton interactions with chromium, iron and nickel at energies up to 3 GeV. The example of neutron displacement cross-section is shown in Fig.3 for iron. Fig.4 presents the cross-sections for various targets at intermediate energies.

III. GAS PRODUCTION CROSS-SECTIONS

The evaluation of hydrogen and helium production cross-sections and yields of protons, deuterons, tritons, ³He-, and ⁴He- nuclei has been performed using results of nuclear model calculations and available experimental data.

TABLE I. Displacement cross-sections (b) for nonelastic interactions of 25 MeV- protons with nickel.

Nuclear model	BCA-MD	NRT
Bertini/Dresner	790	2220
Bertini/ABLA	850	2360
ISABEL/Dresner	760	2160
ISABEL/ABLA	800	2230
CEM03	810	2260
CASCADE	810	2250
DISCA-C	950	2620
Averaged value	820 ± 60	2300 ± 150

TABLE II. Displacement cross-sections (b) for nonelastic interactions of 150 MeV- protons with nickel.

Nuclear model	BCA-MD	NRT
Bertini/Dresner	790	2170
Bertini/ABLA	840	2300
ISABEL/Dresner	770	2120
ISABEL/ABLA	820	2240
CEM03	760	2100
INCL4/Dresner	840	2270
INCL4/ABLA	880	2380
CASCADE	740	2050
DISCA	880	2390
Averaged value	810 ± 50	2220 ± 120

TABLE III. Displacement cross-sections (b) for nonelastic interactions of 1 GeV- protons with nickel.

Nuclear model	BCA-MD	NRT
Bertini/Dresner	830	2340
Bertini/ABLA	910	2570
ISABEL/Dresner	860	2420
ISABEL/ABLA	910	2590
CEM03	830	2290
INCL4/Dresner	1010	2820
INCL4/ABLA	1060	3000
CASCADE	860	2430
Averaged value	910 ± 90	2560 ± 250

TABLE IV. Displacement cross-sections (b) for nonelastic interactions of 3 GeV- protons with nickel.

Nuclear model	BCA-MD	NRT
Bertini/Dresner	630	1730
Bertini/ABLA	740	2020
CEM03	550	1480
INCL4/Dresner	960	2660
INCL4/ABLA	1010	2820
CASCADE	780	2150
Averaged value	780 ± 180	2140 ± 520

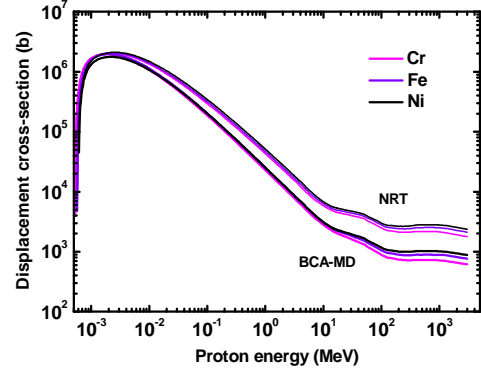


Fig. 2. Displacement cross-sections for chromium, iron, and nickel irradiated with protons with the energy up to 3 GeV obtained using BCA,MD approach and the NRT model.

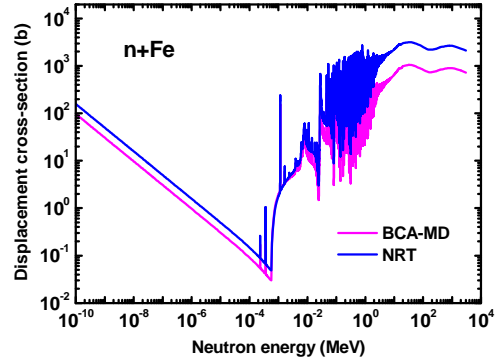


Fig. 3. The displacement cross-section for neutron irradiation of iron at energies up to 3 GeV obtained using BCA,MD approach and the NRT model.

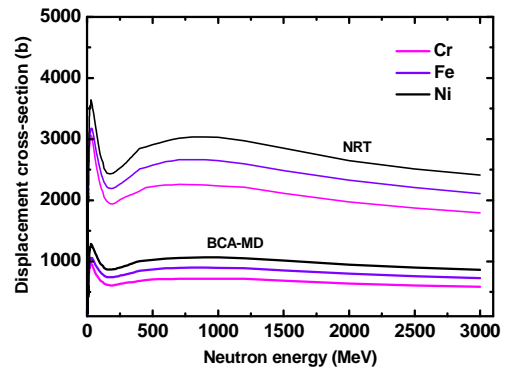


Fig. 4. Neutron displacement cross-sections for chromium, iron, and nickel at intermediate energies obtained using BCA,MD approach and the NRT model.

The calculation of cross-sections was done with the help of various models and codes. The scatter of results was reduced to the “final” calculated curve by the proper weighting. Obtained cross-sections and experimental data were processed using statistical methods implemented in the BEKED computer package¹⁸ to get evaluated cross-sections.

III.A. Brief description of models and codes used for calculations

The calculation of cross-sections was performed using various modifications of the pre-compound, intranuclear cascade, and evaporation models, and models for the simulation of the light cluster emission in nuclear reactions implemented in different computer codes. The brief description of codes applied is presented below.

The ALICE/ASH code: the geometry dependent hybrid model¹⁹⁻²¹ is used for the modeling of the pre-equilibrium particle emission from nuclei. The effective cross-section of nucleon-nucleon interactions in nuclear matter defines transition rates between exciton configurations. The exciton coalescence model^{22,23} and the knock-out model²⁴ are used for the description of the pre-equilibrium complex particle emission. The equilibrium particle emission is described by the Weisskopf-Ewing model without detail consideration of angular momentum.

The TALYS code²⁵: pre-equilibrium exciton model and Hauser-Feshbach model are applied for cross-section calculations. The pre-equilibrium particle emission is described using the two-component exciton model discussed in Ref.26. The contribution of direct processes in the inelastic scattering is calculated using the ECIS code integrated in TALYS. The phenomenological approach from Ref.27 is applied for the calculation of pre-equilibrium emission rates for complex particles. In the present work the calculation of the nuclear level density is performed using the Fermi gas model with the energy dependent nuclear level density parameter²⁸ combined with the “constant temperature” model, as discussed in Ref.25.

The DISCA-C code implements an advanced intranuclear cascade model¹⁷ and the Weisskopf-Ewing model. The INC model simulates nucleon-nucleon and nucleon-cluster interactions. The Weisskopf-Ewing model is used for the simulation of the equilibrium emission of neutrons, protons, deuterons, tritons, ³He nuclei and α -particles. The level density for equilibrium states is calculated by the Fermi gas model at high excitation energies and by the “constant temperature” model at low energies²¹. Inverse reaction cross-sections are evaluated using phenomenological formulas²⁹, which approximate results of optical model calculations.

The CASCADE code: the intranuclear cascade evaporation model¹⁶ is used for the modeling of nuclear

reactions. The specific features of the model include the approximation of the nuclear density by the continuous Woods-Saxon distribution, the use of the “time-like” Monte Carlo technique and the consideration of the effect of nuclear density depletion due to the fast nucleon emission. The contribution of non-equilibrium emission to the yield of light clusters can be calculated using two different approaches: the coalescence model^{30,31} and the method described in Ref.32. In the first case the two step modeling is applied to get an improved energy balance for the non-equilibrium stage of nuclear reactions. The results obtained using both approaches usually are close.

The models from MCNPX package¹⁵. The models “Bertini”, “ISABEL”, and “CEM03” are used with a combination with the pre-equilibrium model. In first two cases so called Multistage Pre-equilibrium Model³³ simulates the fast cluster emission using the old Kalbach-Cline approach³⁴. The calculated d-, t-, ³He-, and ⁴He-production cross-sections are used in the present work only for illustration purposes, because the observed difference between experimental data and calculations seems rather large.

III.B. Use of experimental data

Experimental data for p-, d-, t-, ³He- and α -particle-production cross-sections were taken from EXFOR and the compilation from Ref.35. Charged particle yields measured in the energy interval of secondary particles, which does not cover whole possible energy range of the emission, like Refs.36,37 were corrected using model calculations. Such data were used for the evaluation of gas production cross-sections if the possible contributed error was assumed as “reasonable”. Such data are marked on figures as “corr”.

III.C. Use of data libraries

Data libraries were used as for illustration purposes (ENDF/B-VII, JENDL-HE, TENDL) as for the creation of evaluated data files for energies up to 3 GeV (ENDF/B-VII, EAF-2007, JEFF-3.1.1, Ref.38). In the last case the neutron data for iron and nickel were taken partly from ENDF/B-VII, EAF-2007, and JEFF-3.1.1 and for chromium from Ref.38. The energy range of adopted data concerns mainly low energies of incident neutrons.

III.D. Evaluation of cross-sections

The cross-sections for p-, d-, t-, ³He-, and ⁴He-production were calculated using various nuclear models and codes. Obtained cross-sections and experimental data were used to perform data evaluation applying the statistical methods implemented in the BEKED package¹⁸.

Some examples of calculated and evaluated cross-sections are shown in Figs.5-16. Figures show the proton-

(Figs.5-8), triton- (Figs.9-12), and α -particle (Figs.13-16) production cross-section calculated using TALYS, ALICE/ASH, DISCA-C codes, nuclear models from MCNPX, data from ENDF/B-VII, JENDL-HE, TALYS, and evaluated curves. The good agreement is observed for proton production cross-sections at energies from 20 MeV up to 1 GeV calculated using various INC models except ones including the use of the Dresner model. The reason for the discrepancy of CASCADE, Bertini, and INCL4 calculations above 1 GeV (Fig.7) is not yet clear.

Calculated triton- and α -particle production cross-sections (Figs.9,11,13,15) show more scattering than ones for the proton formation. The libraries data resembles results of calculations than evaluated data (Figs.10,14). The noticeable difference between various calculations is observed also for deuteron- and ^3He - formation cross-sections.

The evaluated data for proton induced reactions were obtained mainly using the results of ALICE/ASH and CASCADE calculations, at lowest energies cross-sections from TALYS calculations, and experimental data. For incident neutrons the well tested and approved data from evaluated data libraries (Section 3.3) were used partly below 150 MeV to obtain evaluated cross-sections in the energy range up to 3 GeV.

IV. EVALUATED DATA FILES

Evaluated data files containing displacement and gas production cross-sections were prepared for natural mixtures of isotopes for chromium, iron, and nickel at incident neutron energies from 10^{-5} eV up to 3 GeV and for incident protons from several eV up to 3 GeV. Two data sets of displacement cross-sections were prepared for each target bases on BCA, MD and the NRT model.

Data were stored using the ENDF-6 format. The standard ENDF-6 sections MT=203-207 of the file MF=3 were used to record proton-, deuteron-, triton-, ^3He -, and ^4He - production cross-sections correspondingly.

Non-standard MT section 900 and 901 were assigned used to store displacement cross-sections obtained using the BCA,MD approach and the NRT model.

IV. CONCLUSION

Displacement cross-sections, proton-, deuteron-, triton-, ^3He -, and ^4He - production cross-sections were obtained for chromium, iron, and nickel for incident neutron and proton energies up to 3 GeV. Various models including the nuclear optical model, the pre-compound exciton model, and the intranuclear cascade evaporation model were used for calculations of cross-section and energy particle and recoil distributions. The binary collision approximation model and results of molecular dynamics simulations were applied to get the number of

generated defects in materials. The evaluation of cross-sections was performed using available experimental data.

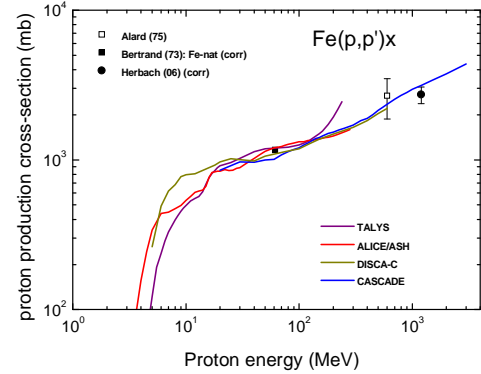


Fig. 5. The cross-section of the proton production in p+Fe interactions calculated using different nuclear models and codes.

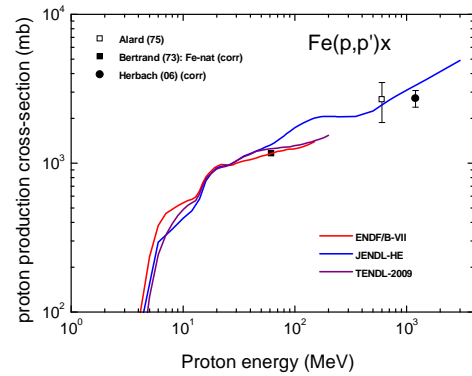


Fig. 6. The cross-section of the proton production in p+Fe interactions taken from evaluated data libraries.

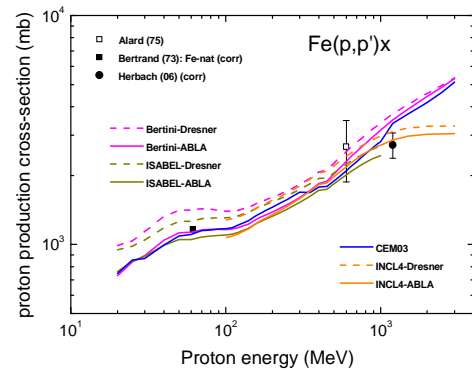


Fig. 7. The cross-section of the proton production in p+Fe interactions calculated using different nuclear models implemented in MCNPX.

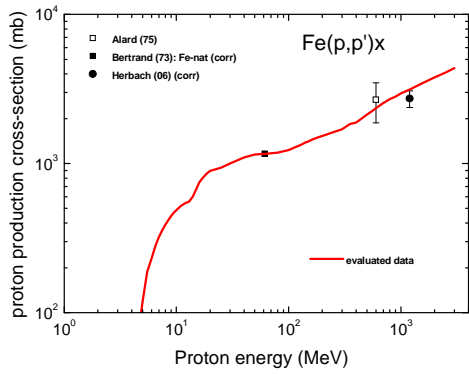


Fig. 8. The cross-section of the proton production in p+Fe interactions evaluated in the present work at energies up to 3 GeV.

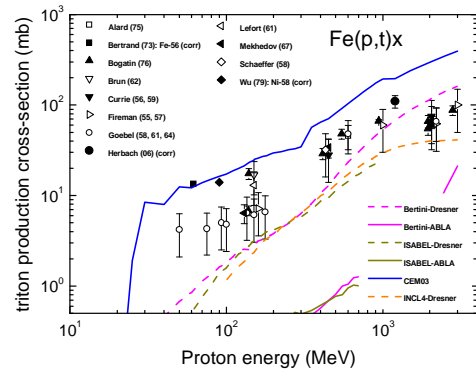


Fig. 11. The cross-section of the triton production in p+Fe interactions calculated using different nuclear models implemented in MCNPX.

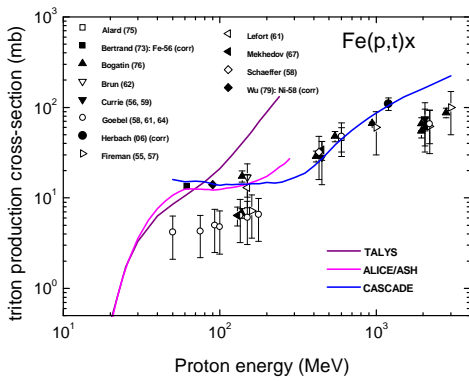


Fig. 9. The cross-section of the triton production in p+Fe interactions calculated using different nuclear models and codes.

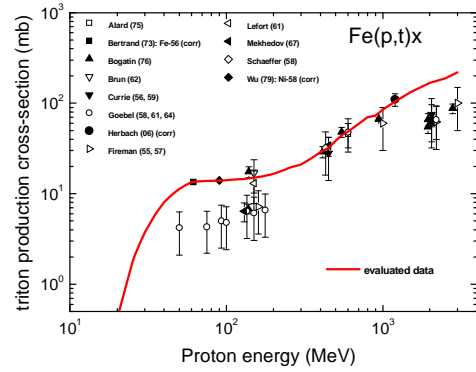


Fig. 12. The cross-section of the triton production in p+Fe interactions evaluated in the present work at energies up to 3 GeV.

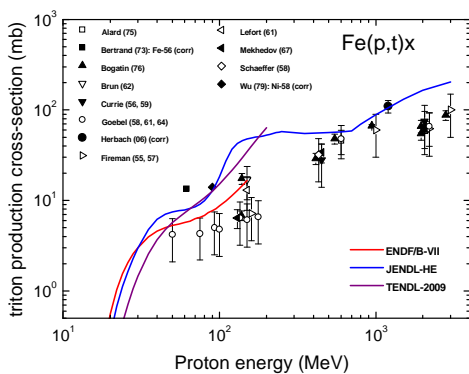


Fig. 10. The cross-section of the triton production in p+Fe interactions taken from evaluated data libraries.

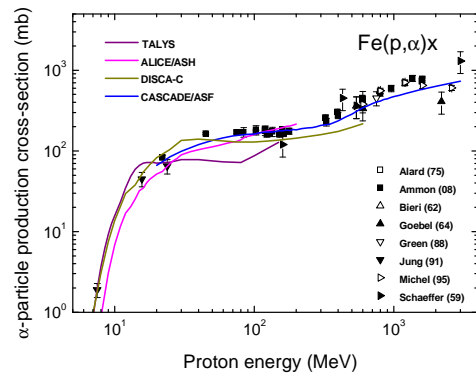


Fig. 13. The cross-section of the α -particle production in p+Fe interactions calculated using different nuclear models and codes.

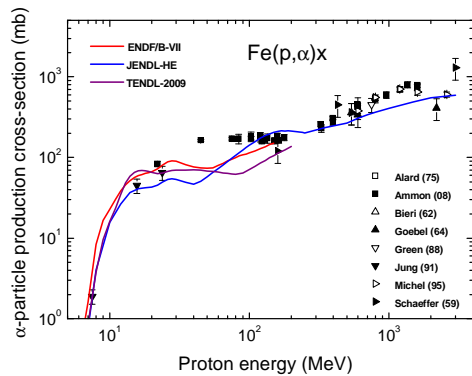


Fig. 14. The cross-section of the α -particle production in p+Fe interactions taken from evaluated data libraries.

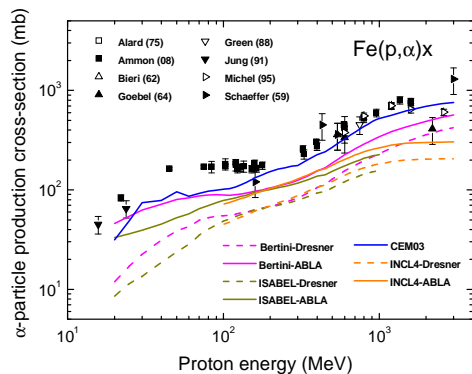


Fig. 15. The cross-section of the α -particle production in p+Fe interactions calculated using different nuclear models implemented in MCNPX.

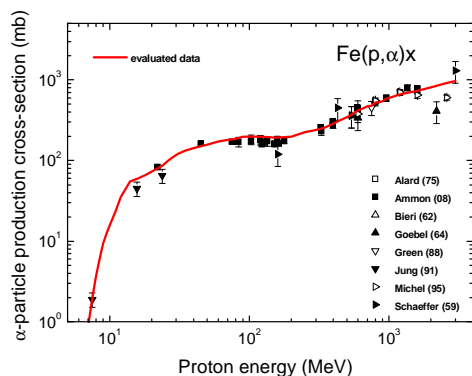


Fig. 16. The cross-section of the α -particle production in p+Fe interactions evaluated in the present work at energies up to 3 GeV.

The data obtained can be applied for the estimation of radiation damage and gas production rates in components of advanced nuclear energy systems. One of the first intended applications is the calculation of radiation damage dose, hydrogen and helium production rates for stainless steel irradiated in European Spallation Source (ESS).

REFERENCES

1. M. J. NORGETT, M. T. ROBINSON, and I. M. TORRENS, "A Proposed Method of Calculating Displacement Dose Rates," *Nucl. Eng. Des.*, **33**, 50 (1975).
2. M. T. ROBINSON, "Basic Physics of Radiation Damage Production," *J. Nucl. Mater.*, 216, 1 (1994).
3. C. H. M. BROEDERS and A. YU. KONOBEYEV, "Evaluation of ^4He Production Cross-Section for Tantalum, Tungsten and Gold Irradiated with Neutrons and Protons at the Energies up to 1 GeV," *Nucl. Instr. Meth. Phys. Res.*, **B234**, 387 (2005).
4. C. H. M. BROEDERS, A. YU. KONOBEYEV, and K. VOUKELATOU, *IOTA - a Code to Study Ion Transport and Radiation Damage in Composite Materials*, FZKA 6984 (2004)
5. C. H. M. BROEDERS and A. YU. KONOBEYEV, "Defect Production Efficiency in Metals under Neutron Irradiation", *J. Nucl. Mater.*, **328**, 197 (2004).
6. C. H. M. BROEDERS and A. YU. KONOBEYEV, "Displacement Cross-Sections for Tantalum and Tungsten Irradiated with Protons at Energies up to 1 GeV," *J. Nucl. Mater.*, **336**, 201 (2005).
7. C. H. M. BROEDERS, A. YU. KONOBEYEV, and C. VILLAGRASA, "Neutron Displacement Cross-Sections for Tantalum and Tungsten at Energies up to 1 GeV", *J. Nucl. Mater.*, **342**, 68 (2005).
8. A. YU. KONOBEYEV, C. H. M. BROEDERS, and U. FISCHER, "Improved Displacement Cross Sections for Structural Materials Irradiated with Intermediate and High Energy Protons," *Proc. 8th Int. Meeting Nucl. Appl. Accelerator Technology*, Pocatello, July 30 - August 2, 2007, p.241.
9. A. YU. KONOBEYEV, U. FISCHER, and L. ZANINI, "New Data Files for the Calculation of Neutron and Proton Induced Radiation Damage Rates in Structural Materials of High Energy Systems", *Proc. 14th Int. Conf. on Emerging Nuclear Energy Systems*, Ericeira, 29th June - 3rd July, 2009, CD
10. K. VÖRTLER, C. BJÖRKAS, D. TERENTYEV, L. MALERBA, and K. NORDLUND, "The Effect of Cr Concentration on Radiation Damage in Fe-Cr Alloys," *J. Nucl. Mat.* **382**, 24 (2008).
11. D. J. BACON, F. GAO, and YU. N. OSETSKY, "The Primary Damage State in fcc, bcc and hcp

- Metals as Seen in Molecular Dynamics Simulations,” *J. Nucl. Mat.*, **276**, 1 (2000).
12. A. J. KONING and J. P. DELAROCHE, “Local and Global Nucleon Optical Models from 1 keV to 200 MeV,” *Nucl. Phys.*, **A713**, 231 (2003).
 13. D. G. MADLAND, “Progress in the Development of Global Medium-Energy Nucleon-Nucleus Optical Model Potentials”, *Proc. Spec. Meeting on the Nucleon Nucleus Optical Model up to 200 MeV*, Bruyères-le-Chatel, November 13-15, 1996 p.129;
 14. A.YU. KONOBEYEV and U. FISCHER, “Uncertainty in Displacement Cross-Section Calculations at Intermediate and High Proton Energies”, *Proc. 4th Workshop Neutron Measurements, Evaluations and Applications*, Prague, October 16 - 18, 2007, p.51.
 15. D. B. PELOWITZ, J. S. HENDRICKS, J. W. DURKEE, M. R. JAMES, M. L. FENSIN, G. W. MCKINNEY, S. G. MASHNIK, and L. S. WATERS, *MCNPX 2.7.A Extensions*, LA-UR-08-07182, (2008).
 16. V.S. BARASHENKOV, “Monte Carlo Simulation of Ionization and Nuclear Processes Initiated by Hadron and Ion Beams in Media,” *Comp. Phys. Comm.*, **126**, 28 (2000) 28.
 17. C. H. M. BROEDERS, A. YU. KONOBEYEV, YU. A. KOROVIN, and V. N. SOSNIN, *DISCA – Advanced Intranuclear Cascade Cluster Evaporation Model Code System for Calculation of Particle Distributions and Cross Sections* FZKA 7221 (2006).
 18. A. YU. KONOBEYEV, U. FISCHER, and P. E. PERESLAVTSEV, “Computational Approach for Evaluation of Nuclear Data Including Covariance Information,” *Proc. Int. Conf. Nuclear Data for Sci. and Technol.*, Jeju Island, Korea, April 26-30, 2010, ND1302
 19. C. H. M. BROEDERS, A. YU. KONOBEYEV, A. YU. KOROVIN, V.P. LUNEV, and M. BLANN, *ALICE/ASH - Pre-Compound and Evaporation Model Code System for Calculation of Excitation Functions, Energy and Angular Distributions of Emitted Particles in Nuclear Reactions at Intermediate Energies*, FZKA 7183 (2006)
 20. M. BLANN and H. K. VONACH, “Global Test of Modified Precompound Decay Models,” *Phys. Rev.*, **C28**, 14 (1983).
 21. M. BLANN, *ALICE-91: Statistical Model Code System with Fission Competition*. RSIC, PSR-14.
 22. A. IWAMOTO and K. HARADA, “Mechanism of Cluster Emission in Nucleon-Induced Preequilibrium Reactions,” *Phys. Rev.*, **C 26**, 1821 (1982).
 23. K. SATO, A. IWAMOTO, and K. HARADA, “Pre-Equilibrium Emission of Light Composite Particles in the Framework of the Exciton Model,” *Phys. Rev.*, **C 28**, 1527 (1983).
 24. A. YU. KONOBEYEV, V. P. LUNEV, and YU. N. SHUBIN, “Pre-Equilibrium Emission of Clusters,” *Acta Physica Slovaca*, **45**, 705 (1995).
 25. A. J. KONING, S. HILAIREY, and M. DUIJVESTIJN, “TALYS-1.0”, 2007.
 26. A. J. KONING, and M. C. DUIJVESTIJN, “A Global Pre-Equilibrium Analysis from 7 to 200 MeV Based on the Optical Model Potential,” *Nucl. Phys.*, **A744** (2004) 15
 27. C. KALBACH, “Preequilibrium Reactions with Complex Particle Channels,” *Phys. Rev.*, **C71**, 034606 (2005)
 28. A. V. IGNATYUK, G. N. SMIRENKIN, and A. S. TISHIN, “Phenomenological Description of the Energy Dependence of the Level Density Parameter,” *Sov. J. Nucl. Phys.*, **21**, 255(1975).
 29. A. CHATTERJEE, K. H. N. MURTHY, S. K. GUPTA, Optical Reaction Cross Sections for Light Projectiles, INDC(IND)-27/GJ, IAEA (1980).
 30. T. C. AWES, S. SAINI, G. POGGI, C. K. GELBKE, D. CHA, R. LEGRAIN, and G. D. WESTFALL, “Light Particle Emission in ¹⁶O-Induced Reactions at 140, 215, and 310 MeV,” *Phys. Rev.* **25**, 2361 (1982).
 31. M. KOZŁOWSKI, H. H. MÜLLER, and R. WAGNER, Analyzing Power and Cross Section of the ⁵⁸Ni, ⁹⁰Zr, ²⁰⁹Bi(\bar{P} , ^{3,4}He X) Reactions in the Continuum Described by the Coalescence Model, *Nucl. Phys.*, **A420**, 1 (1984).
 32. C. H. M. BROEDERS, A. YU. KONOBEYEV, “Helium Production in Solid Target and Metallic Window Materials Irradiated with Intermediate and High Energy Protons”, *J. Nucl. Sci. Technol.*, **42** (2005) 897.
 33. R.E. PRAEL and M. BOZOIAN, *Adaptation of the Multistage Preequilibrium Model for the Monte Carlo Method*, LA-UR-88-3238 (1988).
 34. C. K. CLINE, “Extensions to the pre-equilibrium statistical model and a study of complex particle emission,” *Nucl. Phys.*, **A193**, 417 (1972).
 35. V. S. BARASHENKOV and V. D. TONEEV, *Interaction of High Energy Particles and Atomic Nuclei with Nuclei*, Atomizdat, Moscow, 1972.
 36. F. E. BERTRAND and R. W. PEELLE, “Complete Hydrogen and Helium Particle Spectra from 30- to 60-MeV Proton Bombardment of Nuclei with A=12 to 209 and Comparison with the Intranuclear Cascade Model,” *Phys. Rev. C* **8**, 1045 (1973).
 37. C.-M. HERBACH, D. HILSCHER, U. JAHNKE, V. G. TISHCHENKO, J. GALIN, A. LETOURNEAU, A. PÉGHAIRE, D. FILGES, F. GOLDENBAUM, L. PIENKOWSKI, W. U. SCHRÖDER, and J. TÖKE, “Charged-Particle Evaporation and Pre-Equilibrium Emission in 1.2 GeV Proton-Induced Spallation Reactions,” *Nucl. Phys.*, **A765**, 426 (2006).
 38. P. PERESLAVTSEV, U. FISCHER, and A. KONOBEYEV, “Evaluation of n+Cr-52 Cross Section Data up to 150 MeV Neutron Energy,” *Proc. Int. Conf. Nuclear Data for Sci. and Technol.*, Jeju Island, Korea, April 26-30, 2010, ND1305.